Modulations in motor unit discharge are related to changes in fascicle length during isometric contractions

Eduardo Martinez-Valdes[1], *Francesco Negro[2], Alberto Botter[3,4], *Patricio A Pincheira[5], Giacinto Luigi Cerone[3,4], Deborah Falla[1], Glen A Lichtwark[5], Andrew G Cresswell[5]

[1] Centre of Precision Rehabilitation for Spinal Pain, School of Sport, Exercise and Rehabilitation Sciences, University of Birmingham, United Kingdom.

[2] Department of Clinical and Experimental Sciences, Universita` degli Studi di Brescia, Brescia, Italy.

[3] Laboratory for Engineering of the Neuromuscular System (LISiN), Department of Electronics and Telecommunication, Politecnico di Torino, Torino, Italy.

[4] PoliToBIOMed Lab, Politecnico di Torino, Turin, Italy.

[5]School of Human Movement and Nutrition Sciences, The University of Queensland, Australia

*Authors contributed equally

Running title: Motor unit and fascicle relationships

Keywords: EMG, motor unit, ultrasound, muscle contraction, neuromechanics

Corresponding Author:

Eduardo Martinez-Valdes

Centre of Precision Rehabilitation for Spinal Pain, School of Sport, Exercise and Rehabilitation Sciences, University of Birmingham, United Kingdom.

Edgbaston B15 2TT

e.a.martinezvaldes@bham.ac.uk

+44 0 121 4158187

ABSTRACT

The integration of electromyography (EMG) and ultrasound imaging has provided important information about the mechanisms of muscle activation and contraction. Unfortunately, EMG does not allow an accurate assessment of the interplay between the neural drive received by muscles, changes in fascicle length (FL) and the force/torque produced. We aimed to assess the relationship between modulations in tibialis anterior (TA) motor unit (MU) firing rate, FL and dorsiflexion torque (DT) using ultrasound-transparent high-density EMG electrodes. EMG and ultrasound images were recorded simultaneously from TA, using a 32-electrode silicon matrix, while performing isometric dorsiflexion, at diverse ankle joint positions (0˚ and 30˚ plantar flexion) and torques (20% and 40% of maximum). EMG signals were decomposed into individual MUs and changes in FL were assessed with a fascicle-tracking algorithm. MU firings were converted into a cumulative spike train (CST) that was cross-correlated with DT (CST-DT) and FL (CST-FL). High cross-correlations were found for CST-FL, 0.60 (range: 0.31-0.85) and CST-DT 0.71 (range: 0.31-0.88). Cross-correlation lags revealed that the delay between CST-FL (~75ms) was significantly smaller than CST-DT (~150ms, $p<0.001$). These delays affected the interpretation of MU recruitment/de-recruitment thresholds, with FL showing similar lengths for both recruitment and de-recruitment. This study is the first to demonstrate that changes in TA FL are closely related to both modulations in MU firing frequency and DT. These relationships allow assessment of the interplay between neural drive, muscle contraction and resultant torque, thereby providing a better understanding of the mechanisms responsible for the generation of muscle force.

NEW AND NOTEWORTHY

By employing ultrasound-transparent high-density surface EMG electrodes, we show that modulations in tibialis anterior motor unit discharge rate were closely related to both changes in its fascicle length and resultant torque. These relationships allowed quantifying delays between neural drive and muscle shortening as well as muscle shortening and torque during submaximal isometric contractions, providing an accurate estimation of the time required to generate muscle force and subsequent production of torque via the tendon.

INTRODUCTION

One of the most fundamental issues in motor control is to understand how the nervous system interacts with muscles for the generation of appropriate joint torques and control of movement. While some answers have been obtained from separate studies in the fields of neurophysiology and biomechanics, multiple limitations from previous recording techniques have not allowed to effectively integrate these two disciplines in order to provide clearer information on how neural activity is influenced by muscle mechanics and vice-versa (19, 56). The recent integration of electromyography (EMG) recordings and ultrasound imaging has provided important information about both the mechanisms of muscle activation and contraction (2, 6, 11, 29, 48). These techniques have helped to determine for a given muscle the level of activity related to a given change in fascicle length and allowed the establishment of relationships between active/passive tissue mechanics (i.e., muscle and tendon compliance) and muscle activity. However, there are many limitations to current approaches at linking muscle mechanics with neural drive (number of motor neuron potentials received by muscles

(15, 37)). For example, numerous studies have employed amplitude estimates from bipolar surface EMG recordings in order to assess changes in neural activity and the resultant force produced by muscles (28, 52, 54, 61). Due to many factors such as crosstalk, amplitude cancellation and underlying changes in muscle length and velocity, surface EMG amplitude is unfortunately poorly correlated with the resultant force produced by muscles and therefore cannot be used to directly understand the neural determinants of muscle contractions (16, 17, 42). Furthermore, studies that have examined changes in muscle architecture directly using ultrasound (3, 11, 29, 34) do not often image from the same region as where the EMG is collected (57). Therefore, changes in muscle architecture and/or morphology from nearby or other regions could potentially provide results that are not related from those studied from the region of interest. A few studies have used fine wire electromyography with ultrasound imaging to assess motor unit behaviour in relation to contraction dynamics (32, 46, 47). However, due to its high selectivity, this technique can only sample a small muscle region resulting in relatively low yields of motor units (23), limiting the ability to correlate neural drive received by muscles to the mechanical output.

Ultrasound translucent high-density EMG (HDEMG-US) electrodes have been developed to enable the simultaneous recording of large numbers of motor units and ultrasound images from the same region of muscle during contractions (5). This technique has the potential to improve our understanding of the neuromechanical determinants responsible for the generation of muscle force, however, to-date, this method has not been used to relate single

motor unit discharge characteristics (e.g. blind-source separation decomposition) with fascicle movement tracked from the ultrasound images.

Our primary aim was to assess how tibialis anterior motor unit firing characteristics modulate relative to simultaneous fascicle length changes in different joint positions (short versus long muscle lengths) and at different target torques (20% and 40% of the maximum voluntary contraction, MVC). For this purpose, we examined the relationship between modulations in the motor unit cumulative spike train (CST) along with changes in fascicle length and dorsiflexion torque. We hypothesised that modulations in the CST would be strongly correlated with shortening of the fascicles, which would allow quantification of any delays between motor unit firing, muscle contraction and the torque produced via the tendon. In addition, we also examined differences in recruitment threshold in relation to fascicle length and torque, as possible delays between these signals, might affect the interpretation of motor unit recruitment and de-recruitment thresholds.

METHODS

The study and all procedures were approved by the University of Queensland ethical committee (approval number: 2019001675) and were conducted in accordance with the Declaration of Helsinki. Ten healthy young male volunteers participated [age: mean (SD) 29 (5) years]. Exclusion criteria included any neuromuscular disorder, musculoskeletal injuries such as muscle strain as well as any current or previous history of lower limb pain/injury and be >18 or <35 years of age. Participants were asked to avoid any strenuous activity 24 hours before testing.

Task

114 Participants were seated in a reclined position on the chair of an isokinetic dynamometer
115 (Humac Norm, CSMi Computer Sports Medicine, Stoughton, USA). The right leg (dominant for
116 all participants) was extended and positioned over a support with the knee flexed to 10° (with
117 0° representing full knee extension). To quantify ankle dorsiflexion torque the foot was secured
118 to the dynamometer via non-stretch strapping tape with the approximate centre of rotation of
119 the ankle joint (lateral malleoli) aligned to the axle of the dynamometer. Participants
120 performed sustained and torque-varying (sinusoidal) isometric dorsiflexion contractions at
121 different torque levels at short (ankle at 0° plantar flexion, defined as the sole of the foot being
122 perpendicular to the shank) and long tibialis anterior muscle lengths (ankle at 30° plantar
123 flexion). A schematic describing the setup and measurements is shown in **Figure 1**. The session
124 began with the participants' performing three isometric ankle dorsiflexion MVCs at each ankle
125 angle, where each MVC was separated by 2-min of rest. The order in which the ankle was
126 positioned (short and long tibialis anterior lengths) was randomized. Following the MVC
127 assessment, participants were allowed to practice with visual feedback of their exerted torque
128 (displayed on a computer monitor) performing brief ramp-hold contractions at low torque
129 levels (20% MVC). Then, after 5 min of rest, participants performed ramp-hold (sustained) and
130 torque-varying sinusoidal contractions at 20% or 40% MVC. For sustained isometric
131 contractions, participants were asked to increase their torque at a rate of 10% MVC/s and then
132 to hold the contraction at the target level for 30 s, therefore reaching the 20% MVC target in 2 s
133 and the 40% MVC in 4 s. Two sustained 20% MVC and two sustained 40% MVC contractions
134 were performed. For the torque-varying sinusoidal isometric contractions, the participants also
135 reached an average torque target of 20 and 40% MVC at a rate of 10%MVC/s. However, when

target torque was reached, participants had to track a sinusoidal torque target at a frequency of 0.5 Hz and amplitude modulation of 5% MVC, meaning that torque varied from 17.5% MVC to 22.5% MVC and 37.5% MVC to 42.5% MVC at 20% MVC and 40% MVC, respectively. One sinusoidal contraction per torque level was performed. These sinusoidal contractions aimed to test the ability of both the motor unit decomposition and fascicle tracking algorithms to identify motor units and track changes in fascicle length in conditions where the variability of motor unit firing and fascicle length is increased. All isometric contractions were executed in a randomized order across participants at each muscle length, but the order of the randomization was kept constant between 0˚ and 30˚ of plantar flexion.

Electromyography

Surface EMG signals were recorded from the tibialis anterior muscle using a high-density, 32-channel, HDEMG-US electrode grid (LiSIN, Torino, Italy) (5). Each grid consists of 8 x 4 electrodes (1-mm diameter, 10-mm interelectrode distance in both directions) embedded into a layer of silicon rubber (**Figure 2A)**. The array was located centrally between the proximal and distal tendons of the muscle, with the columns aligned in the direction of the fascicles as confirmed with ultrasound imaging. Skin-electrode contact was made by inserting conductive gel (Sonogel, Bad Camberg, Germany) into the electrode cavities with a mechanical pipette (Eppendorf, Hamburg, Germany) as reported previously (5). Signals were amplified and recorded using a recently developed wireless wearable HDEMG amplifier that contained a 16-bit analogue-digital converter (8) (**Figure 2B),** directly connected the electrode grids, which is ideal when HDEMG measurements are combined with other methods such as ultrasound imaging. For this experiment, data was recorded in monopolar mode at a sampling frequency of

158 2048 Hz, with a gain of 192 ± 1 V/V and a band-pass filter with cut-off frequencies between 10-
159 500 Hz. Torque was also sampled at 2048Hz and recorded through the auxiliary input of the
160 HDEMG amplifier. All EMG and torque data were processed and analysed offline using MATLAB
161 2019b (MathWorks Inc., Natick, MA).

162 *Ultrasonography*

163 Ultrasound images of tibialis anterior fascicles were captured using B-mode ultrasonography (6
164 MHz, 80 frames per second, 60 mm field of view) using a 128-element multi-frequency
165 transducer (LF9-5N60-A3; Telemed, Vilnius, Lithuania) attached to a PC-based ultrasound
166 system (ArtUs EXT-1H scanner; Telemed, Vilnius, Lithuania). A dry HDEMG-US grid (without
167 conductive gel) was first used to find the best alignment of the probe allowing clear
168 visualization of the muscle's fascicles when the probe is placed over the electrodes. Once the
169 optimal position was identified, the skin was marked with an indelible pen. The HDEMG-US
170 electrode grid, with conductive gel, was then positioned over the muscle at the same location
171 and same orientation. The flat-shaped ultrasound transducer was then placed over the
172 electrode grid and firmly strapped over the leg using an elastic bandage to prevent any
173 movement. An example of the setup and an ultrasound image can be seen in **Figure 2B.**

174 *HDEMG and ultrasound synchronization*

175 Torque, HDEMG, and ultrasound data were synchronized utilising an analogue pulse sent from
176 an AD board (Micro 1401-3, Cambridge Electronic Design, Cambridge, UK). The trigger signal
177 was set at 80 Hz and controlled frame by frame the ultrasound recording (i.e. every time the
178 beamformer received a pulse, one frame of ultrasound data was recorded). The same trigger

179 signal was sent to the auxiliary input of the HDEMG device and was aligned offline with the
180 tracked fascicle data (see next section) obtained from the ultrasound files.

181 *Motor unit decomposition and fascicle length tracking*

182 The HDEMG signals were decomposed into motor unit spike trains using an extensively
183 validated blind source separation algorithm, which provides automatic identification of the
184 activity of multiple single motor units (43). Each identified motor unit was assessed for
185 decomposition accuracy with a validated metric (Silhouette, SIL), which represents the
186 sensitivity of the decomposed spike train. Since the identification of motor unit activity with
187 HDEMG-US grids is more challenging due to the lower selectivity of these grids (i.e., 32 channels
188 and inter-electrode distance of 10 mm), an accuracy level of 0.86 SIL (86% of accuracy) was
189 used to approve or discard any motor unit (usual threshold is set at 0.90 SIL (38, 43). Missing
190 pulses producing unphysiological firing rates i.e., inter-spike intervals >250ms, were manually
191 and iteratively included and the pulse train was re-estimated to correct its firing frequency. In
192 cases where the algorithm incorrectly assigned two or three pulses to what was likely only a
193 single discharge time, the operator removed this firing and the final pulse trains were re-
194 estimated as presented previously (1, 4). After this procedure, the average SIL value increased
195 to 0.90 (0.007).

196 Tibialis anterior fascicle length changes were tracked offline by employing custom-made
197 software (Farris & Lichtwark, 2016) utilizing a previously validated Lucas-Kanade optical flow
198 algorithm with affine transformation (24, 25). From each trial, we selected the fascicle in which
199 we were able to visualize ~80% of its length within the field of view of the image. We selected a
200 fascicle from the anterior (superficial) compartment of the tibialis anterior muscle because 1)

201 this was the region of motor unit activity that was likely covered by the HDEMG electrode and
202 2) our preliminary results showed that changes in fascicle length from this region show a cross-
203 correlation coefficient of at least 0.70 with the resultant torque output (see results). Changes in
204 fascicle length were analysed according to shortening length [Δ fascicle length (i.e. difference in
205 fascicle length from rest to target torque (20% MVC)], in order to 1) understand the amount of
206 fascicle shortening required to recruit a motor unit and reach the required torque level (20%
207 MVC and 40% MVC), and 2) to be able to correlate fluctuations in fascicle length with
208 fluctuations in motor unit discharge rate, since absolute changes in fascicle length go in an
209 opposite direction to discharge rate (fascicle length decreases when discharge rate increases,
210 see next section). We also estimated pennation angle as the angle between the fascicle and its
211 insertion into the central aponeurosis (50). The pennation angle was calculated when the
212 muscle was at rest and when the torque was stable during the isometric contractions.

213 *Concurrent motor unit and fascicle length analysis*

214 For sustained isometric contractions, mean discharge rate was calculated from the stable
215 plateau torque region. Motor unit recruitment and de-recruitment thresholds were defined as
216 the ankle dorsiflexion torques (%MVC) or fascicle shortening lengths (Δfascicle length, mm) at
217 the times when the motor units began and stopped discharging action potentials. For these
218 contractions we also tested the possibility to track the same motor units across the two
219 different target torques and muscle lengths, with a previously proposed method based on
220 cross-correlation of 2D motor unit action potentials (MUAPs) (40). In this procedure, matched
221 MUAPs between the two trials (i.e. 20% MVC-0˚ vs 20% MVC-30˚) were visually inspected and
222 the two identified motor units were regarded as the same when they had a cross-correlation

223 coefficient >0.80 (40). Cross-correlation (time domain) analysis was also used to assess the
224 interplay between torque, fascicle length and motor unit firing data. For this purpose, motor
225 unit discharge times were summed to generate a cumulative spike train (CST) as done
226 previously (55). Fascicle length signals were interpolated to 2048Hz to match both motor unit
227 and torque data. After these procedures, CST, fascicle length and torque signals were low-pass
228 filtered (4th order zero-phase Butterworth, 2Hz) and then high-pass filtered (4th order zero-
229 phase Butterworth, 0.75Hz) as presented previously (13). These filtered signals were then cross-
230 correlated to assess similarities in their fluctuations (cross-correlation coefficient) and to
231 calculate any lags between CST vs torque, CST vs fascicle length and fascicle length vs torque.

232 *Statistical Analysis*

233 Unless otherwise indicated, results are expressed as mean and (SD). Normality of the data was
234 assessed with the Shapiro-Wilk test and Sphericity was tested with the Mauchly test.
235 Differences between fascicle parameters (absolute changes in length and pennation angle) at
236 short and long muscle lengths during rest were assessed with paired t-tests. Absolute
237 differences in fascicle length and pennation angle during isometric contractions were assessed
238 with a two-way repeated measures ANOVA, with factors of muscle length (0˚ or 30˚ of plantar
239 flexion) and torque (20 or 40% MVC). For motor unit/Δfascicle length data during isometric
240 contractions, the following statistical tests were employed: 1) two-way repeated measures
241 ANOVA with factors of muscle length and torque to assess differences in discharge rate 2)
242 three-way repeated measures ANOVA with factors of muscle length, torque and signal
243 comparison (CST vs torque, fascicle length vs CST, and torque vs fascicle length) to assess
244 differences in cross-correlation results (correlation coefficient and lag) 3) three-way repeated

measures analysis of variance (ANOVA) with factors of muscle length, torque and recruitment (recruitment vs de-recruitment) to assess differences between recruitment and de-recruitment thresholds (in terms of %MVC torque and Δfascicle length). Finally, all cross-correlation results obtained during sustained and sinusoidal contractions were averaged for each contraction type and compared by paired t-tests. All ANOVA analyses were performed using STATISTICA 12 (Statsoft, Tulsa, USA) and followed by pairwise comparisons with a Student-Newman-Keuls (SNK) post hoc test when significant. Statistical significance was set at $p<0.05$.

RESULTS

Maximal torque, motor unit decomposition and tracking during isometric contractions

The MVC dorsiflexion torque differed at the two ankle positions and was 25.2 (13.2) Nm and 51.8 (12.5) Nm at short (0° plantarflexion) and long (30° plantarflexion) muscle lengths, respectively ($p<0.001$). During both sustained and sinusoidal isometric contractions, an average of 7 (3), 7 (2), 7 (3) and 6 (2) motor units could be identified per participant at 20% MVC-0˚, 20% MVC-30˚, 40% MVC-0˚ and 40% MVC-30˚, respectively. A representative example with the decomposition results from one participant can be seen in **Figure 3.** In this particular example, each motor unit has a clearly distinct MUAP shape (right side of the figure) which allowed accurate identification of discharge times (left side of the figure). An average of 3 (2) motor units could be tracked successfully per participant across the two muscle lengths [2D MUAP cross-correlation coefficient 0.83 (0.03)] and 3 (1) motor units per participant across the two torque levels [2D MUAP cross-correlation coefficient 0.88 (0.05)]. A representative example of the tracking procedure across the two joint angles with the HDEMG-US grids can be seen in **Figure 4**.

267 *Relationships between fascicle length, torque and motor unit discharge rate during isometric*
268 *contractions*

269 Absolute fascicle lengths and pennation angles during rest and isometric contractions at the
270 two different torque targets and two joint angles are presented in **Table 1.** Overall, tibialis
271 anterior fascicles were longer and had smaller pennation angles at 30˚ of plantar flexion at rest
272 and during the contractions ($p<0.001$). Nevertheless, fascicle lengths decreased (torque effect:
273 $p<0.001$, $\eta^2=0.78$) and pennation angles increased (torque effect: $p=0.018$, $\eta^2=0.48$) similarly
274 with increasing dorsiflexion torque at both 0˚ and 30˚ of plantarflexion.

Table 1. Tibialis anterior fascicle length and pennation angles at rest and during sustained isometric dorsiflexion contractions at 20% and 40% MVC at short and long muscle lengths (different joint angles)

	Short (0˚plantar flexion)	**Long (30˚ plantar flexion)**	**P-value**
Pennation angle (°), rest	15.2 (1.7)	12.0 (1.7)	<0.001
Fascicle length (mm), rest	60.2 (8.8)	74.5 (9.1)	<0.001
Pennation angle (°), 20% MVC	19.2 (3.7)	16.9 (3.9)	0.001#
Fascicle length (mm), 20% MVC	52.7 (7.5)	66.3 (9.4)	<0.001*
Pennation angle (°), 40% MVC	20.8 (3.1)	17.4 (4.0)	0.001#
Fascicle length (mm), 40% MVC	50.8 (6.9)	61.9 (7.9)	<0.001*

*Significant effect of torque ($p<0.001$)
#Significant effect of torque ($p=0.018$)

275 Similar to the changes in fascicle length, the tracking of individual motor units across short and
276 long muscle lengths revealed similar discharge rates at the different joint angles (15.3 (2.6) Hz
277 and 14.7 (1.4) Hz at 20% MVC, and 16.7 (2.3) Hz and 17.0 (2.4) Hz at 40% MVC, between 0˚ and
278 30˚ of plantar flexion, respectively, muscle length effect: $p=0.74$, $\eta2=0.047$). However,
279 discharge rate increased with torque (torque effect: $p=0.03$, $\eta^2=0.43$). A representative example
280 of the concurrent assessment of changes in fascicle length, torque and CST can be seen in

Figure 5. Briefly, after the offline identification/tracking of the fascicle (**Figure 5A**), and the identification/editing of the motor unit spike trains and subsequent conversion to CSTs, three signals were obtained: dorsiflexion torque, fascicle length and CST. All these signals were then cross-correlated on the stable torque part of the contraction (**Figure 5B**, upper panel) in order to assess common fluctuations between torque, CST and fascicle length signals. All comparisons showed high levels of cross-correlation (CST vs torque, CST vs fascicle length and fascicle vs torque, **Figure 5B**, bottom panel) and the lags obtained, showed the delay between CST vs torque, CST vs fascicle length and fascicle length vs torque. The cross-correlation results for the group of participants are presented in **Table 2**. Overall, all cross-correlation coefficients ranged from moderate to high (>0.50) showing that there was a clear relationship between CST, fascicle length and torque. It is worth noting that all correlation coefficients were higher during the sinusoidal contractions ($p=0.001$, **Table 2**). Nevertheless, the cross-correlation between CST vs fascicle length was significantly smaller compared to CST vs torque and fascicle length vs torque in both contraction types (signal comparison effect: $p=0.007$, $\eta2=0.427$ and $p<0.0001$, $\eta2=0.846$, for sustained and sinusoidal contractions, respectively). Cross-correlation lags (**Figure 6**) during sustained isometric contractions at 30˚ of plantar flexion (long muscle lengths) were larger than those at 0˚ plantar flexion (short muscle lengths) at both torque levels in all signal comparisons, in both sustained (muscle length effect: $p=0.002$, $\eta2=0.66$) and torque-varying sinusoidal (muscle length effect: $p=0.034$, $\eta2=0.39$) isometric contractions, with no differences between sustained vs sinusoidal isometric lag values.

Table 2. Cross-correlation coefficients for comparisons between cumulative spike train (CST) vs torque, CST vs fascicle length and torque vs fascicle length during isometric contractions.

	Short length 20% MVC	Long Length 20% MVC	Short length 40%MVC	Long length 40% MVC
Steady isometric contractions				
Torque vs CST	0.74 (0.65-0.88)	0.74 (0.62-0.85)	0.74 (0.63-0.85)	0.61 (0.31-0.78)
Fascicle vs CST	0.64 (0.51-0.81)	0.57 (0.31-0.75)	0.63 (0.33-0.85)	0.50 (0.31-0.66)
Torque vs Fascicle	0.71 (0.40-0.88)	0.67 (0.33-0.89)	0.78 (0.33-0.93)	0.72 (0.50-0.91)
Oscillatory isometric contractions				
Torque vs CST	0.78 (0.66-0.89)	0.77 (0.62-0.83)	0.77 (0.66-0.89)	0.66 (0.45-0.82)
Fascicle vs CST	0.71 (0.58-0.86)	0.73 (0.69-0.78)	0.74 (0.60-0.86)	0.62 (0.41-0.75)
Torque vs Fascicle	0.87 (0.75-0.95)	0.89 (0.75-0.95)	0.91 (0.80-0.96)	0.89 (0.77-0.96)

Results are expressed as mean (min-max range).

Variations in tibialis anterior fascicle length and recruitment/de-recruitment thresholds during isometric contractions

Motor unit recruitment and de-recruitment thresholds in terms of both Δfascicle length (mm) and torque (%MVC) are shown for a representative participant in **Figure 7A**. The figure shows that recruitment threshold torque is higher than the torque at de-recruitment, however, the Δfascicle length at which motor units were recruited and de-recruited was similar. This was confirmed in motor units that were tracked across short and long muscle lengths as de-recruitment thresholds were consistently lower when assessed in terms of %MVC torque

325 (recruitment-de-recruitment effect: $p=0.029$, $\eta^2=0.43$, **Figure 7B**) but similar in terms of
326 Δfascicle length (recruitment-de-recruitment effect $p=0.805$, $\eta^2=0.007$, **Figure 7B**,). In addition,
327 although recruitment and de-recruitment thresholds increased in terms %MVC torque across
328 20% and 40% MVC levels (torque effect: $p=0.001$, $\eta^2=0.701$), motor units were recruited and
329 de-recruited at a similar Δfascicle length with increasing torque (torque effect: $p=0.731$,
330 $\eta^2=0.014$). Finally, recruitment-de-recruitment thresholds also increased at long muscle lengths
331 (0° plantar flexion vs 30° plantar flexion) when considered as %MVC torque (muscle length
332 effect: $p<0.001$, $\eta^2=0.77$) but not in terms of Δfascicle length (muscle length effect: $p=0.389$,
333 $\eta^2=0.014$).

334 **DISCUSSION**

335 This is the first study showing that modulations in motor unit discharge rate are closely related
336 to both changes in fascicle length and joint torque during isometric contractions. These
337 relationships allowed us to quantify the delays between motor unit firing activity and fascicle
338 shortening and, fascicle shortening and joint torque during voluntary contractions. By
339 employing this analysis, we demonstrated that the delays between the neural drive and fascicle
340 length or the generated force/torque are larger when the muscle contracts isometrically at
341 longer fascicle lengths (**Figure 6**). In addition, due to the possibility to track motor units across
342 different muscle lengths and target torques, we were also able to show that recruitment and
343 de-recruitment thresholds are similar when considered in terms of fascicle shortening length,
344 meaning that motor units are recruited and de-recruited at the same change in fascicle length,
345 regardless of the joint position or torque exerted. Taken together, the examination of these

346 relationships allows for an accurate assessment of the conversion of neural activity into muscle
347 contractions.
348
349 *CST, fascicle length and torque relationships*
350 A number of studies have shown that fluctuations in firing rate are closely related to the
351 fluctuations in torque/force (14, 42, 55). Considering this observation, we attempted to
352 quantify the level of correlation between fluctuations in firing rate (CST), changes in fascicle
353 length and torque, in order to first, understand whether the information obtained from the
354 identified motor units was linked to the fascicles of the region of interest (CST vs fascicle length
355 correlation) and also to confirm that motor unit firings identified with HDEMG-US grids would
356 be able to predict the fluctuations in torque produced via the tendon. The findings showed that
357 all of the signals compared had moderate to high levels of correlation, confirming that the
358 motor unit data provided a good representation of the changes in fascicle length of the region
359 of interest. Moreover, all correlation levels increased further when greater torque variability
360 was induced during sinusoidal contractions, which shows that motor unit activity is modulated
361 together with changes in fascicle length, providing further confirmation of the close
362 relationship between motor unit discharge and fascicle length. It is important to mention that
363 this greater variability did not affect cross-correlation lags as similar delays were observed in
364 both sustained and oscillatory contractions (**Figure 6**). Recent studies correlating both motor
365 unit firings and torque have shown that the delay between the CST and torque decreases at
366 higher contraction velocities (14, 36). It is likely that the frequency at which the participants
367 matched the sinusoidal target (0.5Hz) was similar to the involuntary torque modulations

368 induced during sustained isometric contractions. Indeed, both Del Vecchio et al. (14) and
369 Martinez-Valdes et al. (36) found even larger delays between CST and torque (~300ms) when
370 the contractions were modulated at slow frequencies (0.5 and 0.25 Hz respectively).
371 Nevertheless, it is likely that the differences in delays between the present research and
372 previous studies is mainly related to variations in the measurement apparatus (i.e., force
373 quantified via a strain gauge versus a torque dynamometer) (9). This provides an advantage in
374 using ultrasound techniques to assess changes in neural activity in relation to muscle contractile
375 dynamics, as these measurements are not affected by differences between dynamometers and
376 could also be used to isolate individual muscle dynamics for joints where multiple muscles
377 actuate the joint.
378 The lower correlation between CST and fascicle length (**Table 2**) during both sustained and
379 sinusoidal isometric contractions could be explained by a number of factors, including the
380 subtle inaccuracies in fascicle length determination from ultrasound imaging and potential
381 mismatches between fibres contributing to CST and the fibres in the imaging region. It is
382 possible that the fascicle tracking or the sampling frequency employed to obtain the images
383 (80Hz) was not sensitive enough to detect small changes in fascicle length, particularly during
384 sustained contractions. However, the sampling frequency is well above the frequency of
385 variation in force during isometric contraction (<5Hz (21)) and tremor (5-13Hz, (60)). Therefore,
386 it is more likely that limitations in imaging the muscle in a single plane and the resolution of the
387 tracking algorithm may contribute to the lower correlations. The depth at which we tracked the
388 fascicles (superficial portion of the tibialis anterior) vs region of motor units recorded may also
389 contribute to discrepancies in the signal correlations; the HDEMG-US electrodes are most likely

390 to only detect motor unit activity of the most superficial motor units (20). If we also consider
391 that blind-source separation motor unit decomposition techniques favour the identification of
392 motor units showing the largest MUAPs and the highest spatial localization on the HDEMG grid
393 (30, 43), it is very likely that the motor units included in the analysis mainly represent the
394 superficial region of tibialis anterior. Nevertheless, it is important to note that we obtained
395 moderate-high cross-correlations between CST and fascicle length during isometric
396 contractions, which demonstrates feasibility of using such approach to understand the link
397 between motor unit firing properties and contraction dynamics.

398 *CST, fascicle length and torque delays*

399 One of the most interesting findings from this study was the possibility of quantifying delays
400 between CST vs. fascicle length and fascicle length vs. torque, during active contractions, which
401 can provide a better understanding of the neuromechanical interactions during movement.
402 Historically, previous studies aiming to quantify the time required to convert neural activity into
403 mechanical output, calculated the time-difference between the onset of force/torque and
404 muscle activation (7) during both voluntary and electrically-induced contractions. This
405 assessment is commonly known as the electromechanical delay, and has provided important
406 information about the time required for a muscle to generate force/torque from a passive
407 state. Since this analysis commonly neglects the lag between the generation of a contraction
408 and the transmission of force to the tendon and then transmission to the measuring apparatus
409 (which generates great variability in results (59)), more recent studies have aimed to quantify
410 these lags by combining conventional bipolar EMG or HDEMG amplitude and ultrasound (3, 58).
411 Similar to the current study, this previous research also revealed that fascicle shortening

412 happens before force/torque is measured (3, 34, 58). However, the magnitude of these delays
413 is considerably smaller than the ones presented herein, with ~6ms (EMG-FL) and ~12ms (EMG-
414 force) of delay for electrically-induced contractions (34, 44) and ~29ms (EMG-FL) and ~50ms
415 (EMG-force) of delay for voluntary contractions (3). Besides the multiple methodological
416 limitations of the aforementioned approaches such as issues with the correct detection of the
417 onset of muscle activation from EMG amplitude (18, 31) and weak correlations between EMG
418 amplitude and force (42), it is difficult to transfer the information obtained from these delays to
419 functional contractions. Moreover, estimates of the electromechanical delay are calculated at a
420 single time-instant when the muscle activates from a passive state, neglecting the influence of
421 the muscle's afferent sensors (i.e. muscle spindle, golgi tendon organ), active motor unit twitch
422 properties and active/passive muscle tissue interactions responsible for the regulation of
423 muscle force during contractions (10). On the contrary, the cross-correlation of signals obtained
424 from HDEMG-US motor unit decomposition and ultrasound could provide a better estimation
425 of these delays, as such assessment considers mechanisms responsible for contraction
426 dynamics (i.e. fascicle length responses to firing rate modulations) rather than just assessing
427 delay differences between signals at contraction onset.
428
429 The longer delays reported in our study are likely due to twitch characteristics of the active
430 motor units (14) and changes in MUAP duration during the contraction. Indeed, a very recent
431 study from Cudicio et al. (10) which employed a new technique of motor unit twitch estimation
432 based on deconvolution of torque and motor unit spike trains reported values of motor unit
433 twitch time-to-peak (~110ms) similar to the delays between CST and torque reported in our

434 study. Moreover, the delays reported in the present investigation between CST and fascicle
435 length (~75ms) are in line with those reported in a previous study from Hamner and Delp (27),
436 where the authors calculated the lag between EMG and simulated muscle activations (when
437 muscle force is produced) during running at 5 m/s. We can therefore speculate that the delays
438 quantified between CST and fascicle length have the potential to explain changes in force
439 transmission during the execution of more functional tasks. However, this would require
440 additional testing of the proposed approach during dynamic contractions.
441
442 *CST, fascicle length and torque delays at different joint positions*
443 Another interesting result obtained from the cross-correlation lags was that both CST vs.
444 fascicle length and fascicle length vs. torque delays increased when the muscle contracted
445 isometrically in a lengthened position (**Figure 6**). Changes in the duration of muscle-fibre twitch
446 force and muscle-tendon compliance at larger muscle lengths likely influenced these delays. To
447 provide support to the first observation, several studies have reported that muscle twitches are
448 significantly larger (greater contraction and half-relaxation times) when the muscle is
449 lengthened (10, 35, 53). Therefore, it is very likely that an increase in the overall duration of the
450 motor unit responses at longer lengths is the reason for the more delayed muscle contraction
451 and transmission of force to the tendon observed at the two submaximal normalized torque
452 targets (20 and 40% MVC). In addition, changes in tendon and aponeurosis elasticity during
453 lengthening could also reduce the amount of neural drive required to activate the muscle (33,
454 41, 49) and potentially increase the delays between signals. Nevertheless, the assessment of
455 both motor unit contractile properties and the effect of passive structural properties of the

456 muscle on motor unit behaviour needs to be confirmed in future investigations. The assessment
457 of these delays holds great potential in both healthy populations (e.g. aging) and patients (e.g.
458 cerebral palsy), as they could help to quantify impairments in force transmission, when muscles
459 have altered architecture (e.g. muscle contractures or sarcopenia).
460
461 *Recruitment vs. De-recruitment threshold discrepancies*
462 The discrepancy between %MVC vs fascicle length recruitment and de-recruitment thresholds
463 was an interesting observation. Motor unit studies typically use torque/force to assume
464 changes in muscle behaviour, however, delays between motor unit firing and torque due to
465 force transmission delays (along muscle/tendon and also within dynamometer) could create
466 offsets when comparing recruitment (torque rise) vs decruitment (torque drop) thresholds. The
467 findings from this study suggest that it is important to consider these delays when interpreting
468 recruitment and de-recruitment results from torque/force signals since we were able to
469 observe that recruitment and de-recruitment thresholds differed when quantified as % MVC
470 torque (recruitment threshold was higher than the de-recruitment threshold) but were similar
471 when quantified in terms of fascicle length. To our knowledge, this is the first study showing
472 this discrepancy. Moreover, we were able to observe that the length at which a motor unit was
473 recruited and de-recruited was maintained across joint angles and torque levels. Fascicle
474 shortening preceded torque generation (as expected), but fascicles returned to resting values
475 after the dorsiflexion torque returned to 0 Nm. This means that during the ramp-down phase of
476 the contraction, there is a time-point where the muscle returns passively to its original length
477 (**Figure 7**). This can explain why many studies show lower torque values for de-recruitment than

478 recruitment when considered as %MVC torque or absolute torque (12, 39, 51) and emphasizes
479 the need to interpret recruitment vs de-recruitment relationships with caution, when
480 quantified from the torque produced at the dynamometer. Interestingly, similar divergences
481 were recently reported when considering recruitment and de-recruitment in terms of joint
482 angle or fascicle length during isometric plantarflexion contractions at varying knee-joint angles
483 (32).
484
485
486
487 *Limitations and future developments*
488 In this study we were able identify an average of 7 motor units across contractions, which is
489 lower than the number of units identified with non-transparent HDEMG electrodes, where
490 approximately 15 to 20 motor units can be identified on the tibialis anterior muscle on average
491 per participant (39). These differences can be attributed to a number of factors. First, the grid
492 of electrodes employed in the current study contained 32 electrodes vs. the 64 electrodes
493 conventionally employed to decompose EMG signals. It has been shown that a larger number of
494 channels enhances the spatial identification of MUAPs and therefore improves the separation
495 of the multiple motor unit sources from the HDEMG with blind-source separation methods (22,
496 43). Second, the inter-electrode distance of the HDEMG-US grid (10mm) is less selective than
497 the 64-channel grids (8mm) commonly employed to decompose motor unit activity, which can
498 again influence the separation of MUAPs from the HDEMG. Therefore, improvements in
499 electrode construction will likely increase the number of motor units identified with HDEMG-

US. Nevertheless, it is important to mention that the cross-correlation between motor unit discharge rate and torque was high (~0.70) and similar to the values reported in previous studies (14, 42, 55). As mentioned previously, muscle fascicle imaging using ultrasound also has some limitations in terms of the resolution of the image limiting the tracking of small changes in fascicle length, as well as the limitation of only being able to image one plane of the muscle. Improvements in ultrasound probe construction and/or the addition of another ultrasound probe in a different portion of the electrode grid would likely help to improve estimations of changes in fascicle length during isometric contractions. Finally, it is worth mentioning that the accurate assessment of motor unit and fascicle data across torque levels and joint positions, opens up the opportunity to explore more diverse isometric contraction models (i.e., ballistic contractions or faster sinusoidal contractions) and shortening and lengthening contractions. Our present results were not affected by more dynamic variations in isometric torque and the tracking of motor units across joint angles revealed that MUAPs did not change substantially within the range of motion investigated (**Figure 4**). Very recent studies employing HDEMG recordings (without ultrasound) have successfully identified motor units during shortening and lengthening contractions (26, 45), therefore, it is very likely that future studies assessing changes in motor unit activity and fascicle length will be able to assess these interactions during dynamic conditions.

Conclusion

In conclusion, this study shows that modulations in motor unit firing rate are closely related to changes in fascicle length during isometric contractions. The determination of these

522 relationships allows quantifying delays between MUAP propagation, muscle contraction and
523 subsequent transmission of force to the tendon during sustained and functional torque
524 modulation, providing a better representation of the mechanisms responsible for the control of
525 muscle force during active contractions.
526

527 **ACKNOWLEDGEMENTS**

528 This study was partially funded with the University of Birmingham International Engagement
529 Fund (BIEF) awarded to E.M.-V.
530
531

532 **DISCLOSURES**

533 No conflicts of interest, financial or otherwise, are declared by the authors.
534

535 **Author contributions**

536 Experiments were performed at the School of Human Movement and Nutrition Sciences,
537 University of Queensland, Queensland, Australia. E.M.-V. designed research; E.M.-V and P.P.
538 performed experiments; E.M.-V. and F.N. analysed the data; E.M.-V., F.N., A.B., G.C., D.F., P.P.,
539 G.L. and A.C. interpreted the data and contributed to the drafting of the article. All authors
540 have read and approved final submission.
541

542 **REFERENCES**

1. **Afsharipour B, Manzur N, Duchcherer J, Fenrich KF, Thompson CK, Negro F, Quinlan KA, Bennett DJ, and Gorassini MA**. Estimation of self-sustained activity produced by persistent inward currents using firing rate profiles of multiple motor units in humans. *J Neurophysiol* 124: 63-85, 2020.
2. **Barber LA, Barrett RS, Gillett JG, Cresswell AG, and Lichtwark GA**. Neuromechanical properties of the triceps surae in young and older adults. *Exp Gerontol* 48: 1147-1155, 2013.
3. **Begovic H, Zhou GQ, Li T, Wang Y, and Zheng YP**. Detection of the electromechanical delay and its components during voluntary isometric contraction of the quadriceps femoris muscle. *Front Physiol* 5: 494, 2014.
4. **Boccia G, Martinez-Valdes E, Negro F, Rainoldi A, and Falla D**. Motor unit discharge rate and the estimated synaptic input to the vasti muscles is higher in open compared with closed kinetic chain exercise. *J Appl Physiol (1985)* 127: 950-958, 2019.
5. **Botter A, Vieira TM, Loram ID, Merletti R, and Hodson-Tole EF**. A novel system of electrodes transparent to ultrasound for simultaneous detection of myoelectric activity and B-mode ultrasound images of skeletal muscles. *J Appl Physiol (1985)* 115: 1203-1214, 2013.
6. **Brown SH, and McGill SM**. A comparison of ultrasound and electromyography measures of force and activation to examine the mechanics of abdominal wall contraction. *Clin Biomech (Bristol, Avon)* 25: 115-123, 2010.
7. **Cavanagh PR, and Komi PV**. Electromechanical delay in human skeletal muscle under concentric and eccentric contractions. *Eur J Appl Physiol Occup Physiol* 42: 159-163, 1979.
8. **Cerone GL, Botter A, and Gazzoni M**. A Modular, Smart, and Wearable System for High Density sEMG Detection. *IEEE Trans Biomed Eng* 66: 3371-3380, 2019.
9. **Corcos DM, Gottlieb GL, Latash ML, Almeida GL, and Agarwal GC**. Electromechanical delay: An experimental artifact. *J Electromyogr Kinesiol* 2: 59-68, 1992.
10. **Cudicio A, Martinez-Valdes E, Cogliati M, Orizio C, and Negro F**. The force-generation capacity of the tibialis anterior muscle at different muscle-tendon lengths depends on its motor unit contractile properties. *Eur J Appl Physiol* 2021.
11. **Day JT, Lichtwark GA, and Cresswell AG**. Tibialis anterior muscle fascicle dynamics adequately represent postural sway during standing balance. *J Appl Physiol (1985)* 115: 1742-1750, 2013.
12. **De Luca CJ**. Control properties of motor units. *J Exp Biol* 115: 125-136, 1985.
13. **De Luca CJ, and Erim Z**. Common drive of motor units in regulation of muscle force. *Trends Neurosci* 17: 299-305, 1994.
14. **Del Vecchio A, Ubeda A, Sartori M, Azorin JM, Felici F, and Farina D**. Central nervous system modulates the neuromechanical delay in a broad range for the control of muscle force. *J Appl Physiol (1985)* 125: 1404-1410, 2018.
15. **Dideriksen JL, Enoka RM, and Farina D**. Neuromuscular adjustments that constrain submaximal EMG amplitude at task failure of sustained isometric contractions. *J Appl Physiol (1985)* 111: 485-494, 2011.
16. **Dideriksen JL, and Farina D**. Amplitude cancellation influences the association between frequency components in the neural drive to muscle and the rectified EMG signal. *PLoS Comput Biol* 15: e1006985, 2019.
17. **Dideriksen JL, Negro F, Falla D, Kristensen SR, Mrachacz-Kersting N, and Farina D**. Coherence of the Surface EMG and Common Synaptic Input to Motor Neurons. *Front Hum Neurosci* 12: 207, 2018.
18. **Dieterich AV, Botter A, Vieira TM, Peolsson A, Petzke F, Davey P, and Falla D**. Spatial variation and inconsistency between estimates of onset of muscle activation from EMG and ultrasound. *Sci Rep* 7: 42011, 2017.
19. **Enoka RM**. Biomechanics and neuroscience: a failure to communicate. *Exerc Sport Sci Rev* 32: 1-3, 2004.

20. **Farina D, Cescon C, and Merletti R**. Influence of anatomical, physical, and detection-system parameters on surface EMG. *Biol Cybern* 86: 445-456, 2002.
21. **Farina D, and Negro F**. Common synaptic input to motor neurons, motor unit synchronization, and force control. *Exerc Sport Sci Rev* 43: 23-33, 2015.
22. **Farina D, Negro F, Gazzoni M, and Enoka RM**. Detecting the unique representation of motor-unit action potentials in the surface electromyogram. *J Neurophysiol* 100: 1223-1233, 2008.
23. **Farina D, Negro F, Muceli S, and Enoka RM**. Principles of Motor Unit Physiology Evolve With Advances in Technology. *Physiology (Bethesda)* 31: 83-94, 2016.
24. **Farris DJ, and Lichtwark GA**. UltraTrack: Software for semi-automated tracking of muscle fascicles in sequences of B-mode ultrasound images. *Comput Methods Programs Biomed* 128: 111-118, 2016.
25. **Gillett JG, Barrett RS, and Lichtwark GA**. Reliability and accuracy of an automated tracking algorithm to measure controlled passive and active muscle fascicle length changes from ultrasound. *Comput Methods Biomech Biomed Engin* 16: 678-687, 2013.
26. **Glaser V, and Holobar A**. Motor Unit Identification From High-Density Surface Electromyograms in Repeated Dynamic Muscle Contractions. *IEEE Trans Neural Syst Rehabil Eng* 27: 66-75, 2019.
27. **Hamner SR, and Delp SL**. Muscle contributions to fore-aft and vertical body mass center accelerations over a range of running speeds. *J Biomech* 46: 780-787, 2013.
28. **Heintz S, and Gutierrez-Farewik EM**. Static optimization of muscle forces during gait in comparison to EMG-to-force processing approach. *Gait Posture* 26: 279-288, 2007.
29. **Hodges PW, Pengel LH, Herbert RD, and Gandevia SC**. Measurement of muscle contraction with ultrasound imaging. *Muscle Nerve* 27: 682-692, 2003.
30. **Holobar A, and Farina D**. Blind source identification from the multichannel surface electromyogram. *Physiol Meas* 35: R143-165, 2014.
31. **Hug F, Lacourpaille L, and Nordez A**. Electromechanical delay measured during a voluntary contraction should be interpreted with caution. *Muscle Nerve* 44: 838-839, 2011.
32. **Lauber B, Lichtwark GA, and Cresswell AG**. Reciprocal activation of gastrocnemius and soleus motor units is associated with fascicle length change during knee flexion. *Physiol Rep* 2: 2014.
33. **Lichtwark GA, and Wilson AM**. Is Achilles tendon compliance optimised for maximum muscle efficiency during locomotion? *J Biomech* 40: 1768-1775, 2007.
34. **Ling YT, Ma CZ, Shea QTK, and Zheng YP**. Sonomechanomyography (SMMG): Mapping of Skeletal Muscle Motion Onset during Contraction Using Ultrafast Ultrasound Imaging and Multiple Motion Sensors. *Sensors (Basel)* 20: 2020.
35. **Marsh E, Sale D, McComas AJ, and Quinlan J**. Influence of joint position on ankle dorsiflexion in humans. *J Appl Physiol Respir Environ Exerc Physiol* 51: 160-167, 1981.
36. **Martinez-Valdes E, Negro F, Arvanitidis M, Farina D, and Falla D**. Pain-induced changes in motor unit discharge depend on recruitment threshold and contraction speed. *J Appl Physiol (1985)* 2021.
37. **Martinez-Valdes E, Negro F, Falla D, De Nunzio AM, and Farina D**. Surface electromyographic amplitude does not identify differences in neural drive to synergistic muscles. *J Appl Physiol (1985)* 124: 1071-1079, 2018.
38. **Martinez-Valdes E, Negro F, Falla D, Dideriksen JL, Heckman CJ, and Farina D**. Inability to increase the neural drive to muscle is associated with task failure during submaximal contractions. *J Neurophysiol* 124: 1110-1121, 2020.
39. **Martinez-Valdes E, Negro F, Farina D, and Falla D**. Divergent response of low- versus high-threshold motor units to experimental muscle pain. *J Physiol* 598: 2093-2108, 2020.

40. **Martinez-Valdes E, Negro F, Laine CM, Falla D, Mayer F, and Farina D**. Tracking motor units longitudinally across experimental sessions with high-density surface electromyography. *J Physiol* 595: 1479-1496, 2017.
41. **Mayfield DL, Cresswell AG, and Lichtwark GA**. Effects of series elastic compliance on muscle force summation and the rate of force rise. *J Exp Biol* 219: 3261-3270, 2016.
42. **Negro F, Holobar A, and Farina D**. Fluctuations in isometric muscle force can be described by one linear projection of low-frequency components of motor unit discharge rates. *J Physiol* 587: 5925-5938, 2009.
43. **Negro F, Muceli S, Castronovo AM, Holobar A, and Farina D**. Multi-channel intramuscular and surface EMG decomposition by convolutive blind source separation. *J Neural Eng* 13: 026027, 2016.
44. **Nordez A, Gallot T, Catheline S, Guevel A, Cornu C, and Hug F**. Electromechanical delay revisited using very high frame rate ultrasound. *J Appl Physiol (1985)* 106: 1970-1975, 2009.
45. **Oliveira AS, and Negro F**. Neural Control of Matched Motor Units during Muscle Shortening and Lengthening at Increasing Velocities. *J Appl Physiol (1985)* 2021.
46. **Pasquet B, Carpentier A, and Duchateau J**. Change in muscle fascicle length influences the recruitment and discharge rate of motor units during isometric contractions. *J Neurophysiol* 94: 3126-3133, 2005.
47. **Pasquet B, Carpentier A, and Duchateau J**. Specific modulation of motor unit discharge for a similar change in fascicle length during shortening and lengthening contractions in humans. *J Physiol* 577: 753-765, 2006.
48. **Pincheira PA, Hoffman BW, Cresswell AG, Carroll TJ, Brown NAT, and Lichtwark GA**. The repeated bout effect can occur without mechanical and neuromuscular changes after a bout of eccentric exercise. *Scand J Med Sci Sports* 28: 2123-2134, 2018.
49. **Raiteri BJ, Cresswell AG, and Lichtwark GA**. Muscle-tendon length and force affect human tibialis anterior central aponeurosis stiffness in vivo. *Proc Natl Acad Sci U S A* 115: E3097-E3105, 2018.
50. **Reeves ND, and Narici MV**. Behavior of human muscle fascicles during shortening and lengthening contractions in vivo. *J Appl Physiol (1985)* 95: 1090-1096, 2003.
51. **Romaiguere P, Vedel JP, and Pagni S**. Comparison of fluctuations of motor unit recruitment and de-recruitment thresholds in man. *Exp Brain Res* 95: 517-522, 1993.
52. **Son J, Hwang S, and Kim Y**. An EMG-based muscle force monitoring system. *Journal of Mechanical Science and Technology* 24: 2099-2105, 2010.
53. **Stephens JA, Reinking RM, and Stuart DG**. The motor units of cat medial gastrocnemius: electrical and mechanical properties as a function of muscle length. *J Morphol* 146: 495-512, 1975.
54. **Suzuki R, Kanehisa H, Washino S, Watanabe H, Shinohara M, and Yoshitake Y**. Reconstruction of net force fluctuations from surface EMGs of multiple muscles in steady isometric plantarflexion. *Exp Brain Res* 239: 601-612, 2021.
55. **Thompson CK, Negro F, Johnson MD, Holmes MR, McPherson LM, Powers RK, Farina D, and Heckman CJ**. Robust and accurate decoding of motoneuron behaviour and prediction of the resulting force output. *J Physiol* 596: 2643-2659, 2018.
56. **Tytell ED, Holmes P, and Cohen AH**. Spikes alone do not behavior make: why neuroscience needs biomechanics. *Curr Opin Neurobiol* 21: 816-822, 2011.
57. **Vieira TM, and Botter A**. The Accurate Assessment of Muscle Excitation Requires the Detection of Multiple Surface Electromyograms. *Exerc Sport Sci Rev* 49: 23-34, 2021.
58. **Waasdorp R, Mugge W, Vos HJ, Groot JHd, Verweij MD, Jong Nd, Schouten AC, and Daeichin V**. Combining Ultrafast Ultrasound and High-Density EMG to Assess Local Electromechanical Muscle Dynamics: A Feasibility Study. *IEEE Access* 9: 45277-45288, 2021.
59. **Yavuz SU, Sendemir-Urkmez A, and Turker KS**. Effect of gender, age, fatigue and contraction level on electromechanical delay. *Clin Neurophysiol* 121: 1700-1706, 2010.

684 60. **Yavuz US, Negro F, Falla D, and Farina D**. Experimental muscle pain increases variability of
685 neural drive to muscle and decreases motor unit coherence in tremor frequency band. *J Neurophysiol*
686 114: 1041-1047, 2015.
687 61. **Yoshitake Y, and Shinohara M**. Low-frequency component of rectified EMG is temporally
688 correlated with force and instantaneous rate of force fluctuations during steady contractions. *Muscle*
689 *Nerve* 47: 577-584, 2013.

690

691

692

693

694

695 **FIGURE LEGENDS**

696 **Figure 1.** Study schematic. MVC, maximum voluntary contraction torque.

697 **Figure 2.** High-density surface electromyography (HDEMG) ultrasound-transparent electrodes.
698 A) Back (up) and front (down) of the 32-channel (10 mm inter-electrode distance) electrode
699 grid. B) HDEMG electrode grid with 32-channel HDEMG amplifier (connected on top of the
700 electrode) and flat ultrasound probe can be seen on the left. Ultrasound image of proximal
701 tibialis anterior muscle can be seen on the right. Note the quality of the image with accurate
702 visualization of fascicles and, superficial, intermediate and deep aponeuroses.

703 **Figure 3.** Motor unit identification during isometric contractions. A total of 11 motor units
704 (MUs) were decomposed from the HDEMG signals in a representative participant during an
705 isometric contraction at 20% of the maximum voluntary torque (0° of plantarflexion).
706 Instantaneous firing rate with torque profile can be seen on the left of the figure while 2D
707 motor unit action potentials (MUAPs) from each of these motor units can be seen on the right
708 of the figure. Note the clear differences in MUAP shape for each of the identified units.

709 **Figure 4.** Motor unit tracking. A representative example of a motor unit that was tracked across
710 two-plantarflexion angles at 20% MVC can be seen on the figure. For this motor unit, the action
711 potentials (single differential) had a cross correlation coefficient of 0.90 across angles. The
712 instantaneous firing rate of this unit can be seen on the bottom of the figure.

713 **Figure 5.** Fascicle length tracking procedure and correlation with torque and motor unit data. A)
714 A tibialis anterior ultrasound image and a fascicle of interest (red) can be seen on top of the
715 figure. The length data obtained from the tracking of this fascicle was then correlated with
716 torque and cumulative spike train (CST) signals (bottom). Fascicle length data is presented as
717 the amount of shortening from rest to target torque (fascicle length during rest minus fascicle
718 length reached at target torque). Note that fascicle shortening precedes the generation of
719 torque during the ramp-up phase of the contraction and then returns to baseline values after
720 the torque signal returns to zero. The steady torque part that was selected to correlate signals
721 is inside the rectangle. B) Common fluctuations from the three generated signals (torque, CST
722 and fascicle length) in the steady-torque part of the contraction can be seen on top of the
723 figure. Cross-correlation and lag (delay, ms) results between CST vs torque, CST vs fascicle
724 length (fascicle) and fascicle vs torque can be seen on the bottom of the figure.

725 **Figure 6.** Cross-correlation lag (delay) results during sustained and sinusoidal isometric
726 contractions. Delays between cumulative spike train (CST) vs torque, CST vs fascicle length
727 (fascicle) and fascicle vs torque can be seen for sustained (A) and sinusoidal (B) isometric
728 contractions at 0° and 30° of plantarflexion at 20% MVC and 40% MVC. *, significant effect of
729 joint angle ($p<0.05$).

730 **Figure 7.** Recruitment and de-recruitment thresholds in relation to torque and fascicle length. A
731 representative example of recruitment and de-recruitment threshold of a motor unit in relation
732 to torque and fascicle length can be seen on the left of the figure. The recruitment threshold for
733 this unit was higher than the de-recruitment threshold when calculated as %MVC torque (green
734 dashed line) but similar when calculated as fascicle shortening length (blue dashed line).
735 Fascicle length data is presented as the amount of shortening from rest to target torque
736 (fascicle length during rest-fascicle length reached at target torque). The same results can be
737 appreciated by the group of participants on the right of the figure as recruitment thresholds are
738 consistently higher than de-recruitment thresholds across target torques and angles when
739 considered as %MVC torque (upper right) but similar when calculated from fascicle length data
740 (lower right). *, significant effect of recruitment-de-recruitment ($p<0.05$). #, significant effect of
741 joint angle ($p<0.05$). Ψ, significant effect of torque ($p<0.05$).

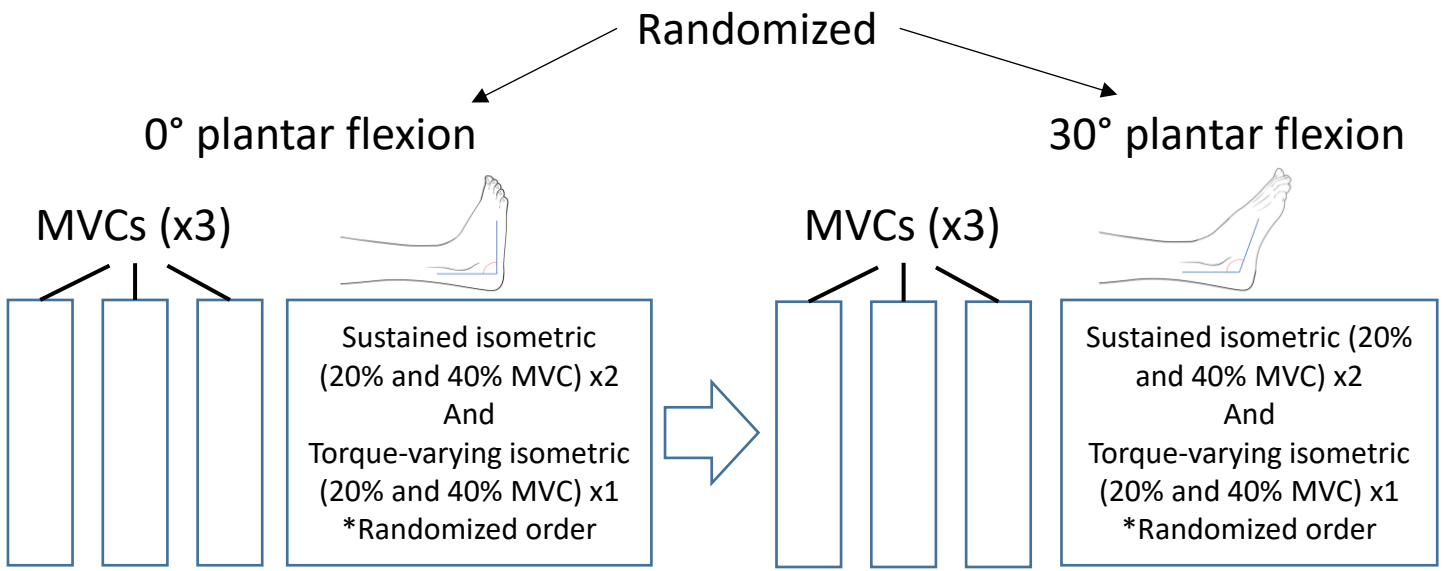
Randomized
0° plantar flexion
30° plantar flexion
MVCs (x3)
Sustained isometric
(20% and 40% MVC) x2
And
Torque-varying isometric
(20% and 40% MVC) x1
*Randomized order
MVCs (x3)
Sustained isometric (20%
and 40% MVC) x2
And
Torque-varying isometric
(20% and 40% MVC) x1
*Randomized order

A)

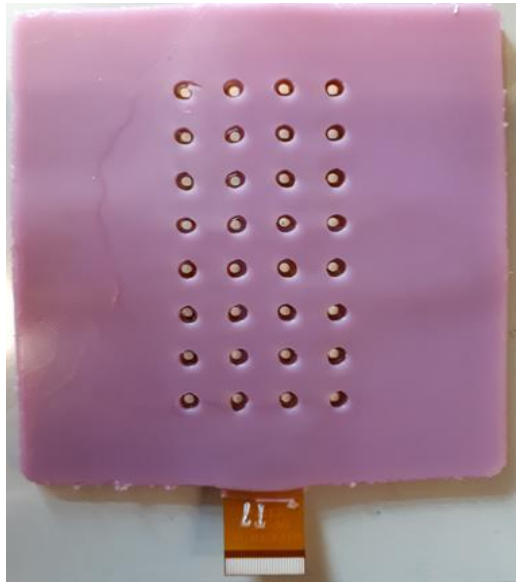

B)

Distal Proximal

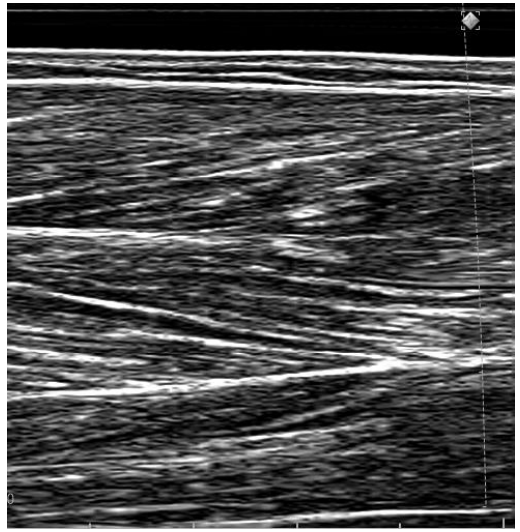

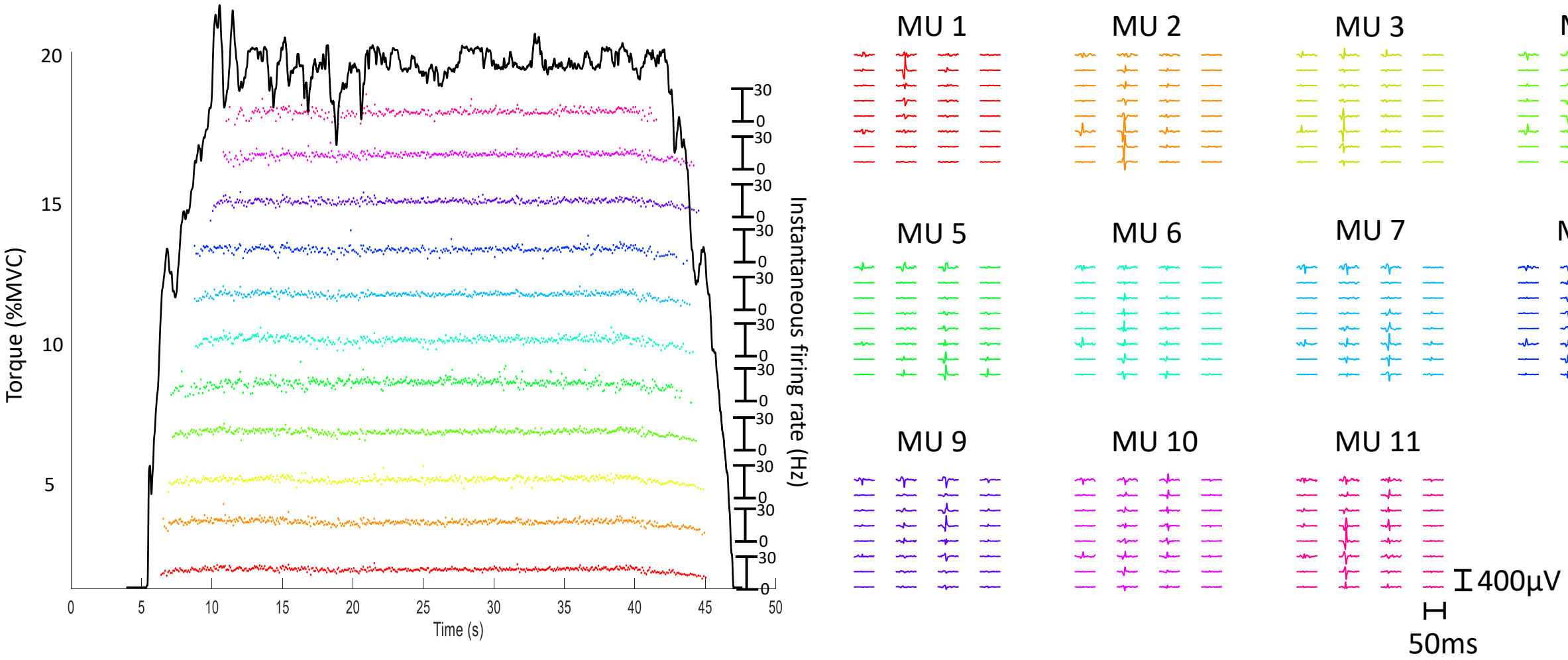
Torque (%MVC)
20
15
10
5
0
5
10
15
20
25
30
35
40
45
50
Time (s)
Instantaneous firing rate (Hz)
30
0
MU 1
MU 2
MU 3
MU 4
MU 5
MU 6
MU 7
MU 8
MU 9
MU 10
MU 11
400µV
50ms

Cross correlation = 0.90

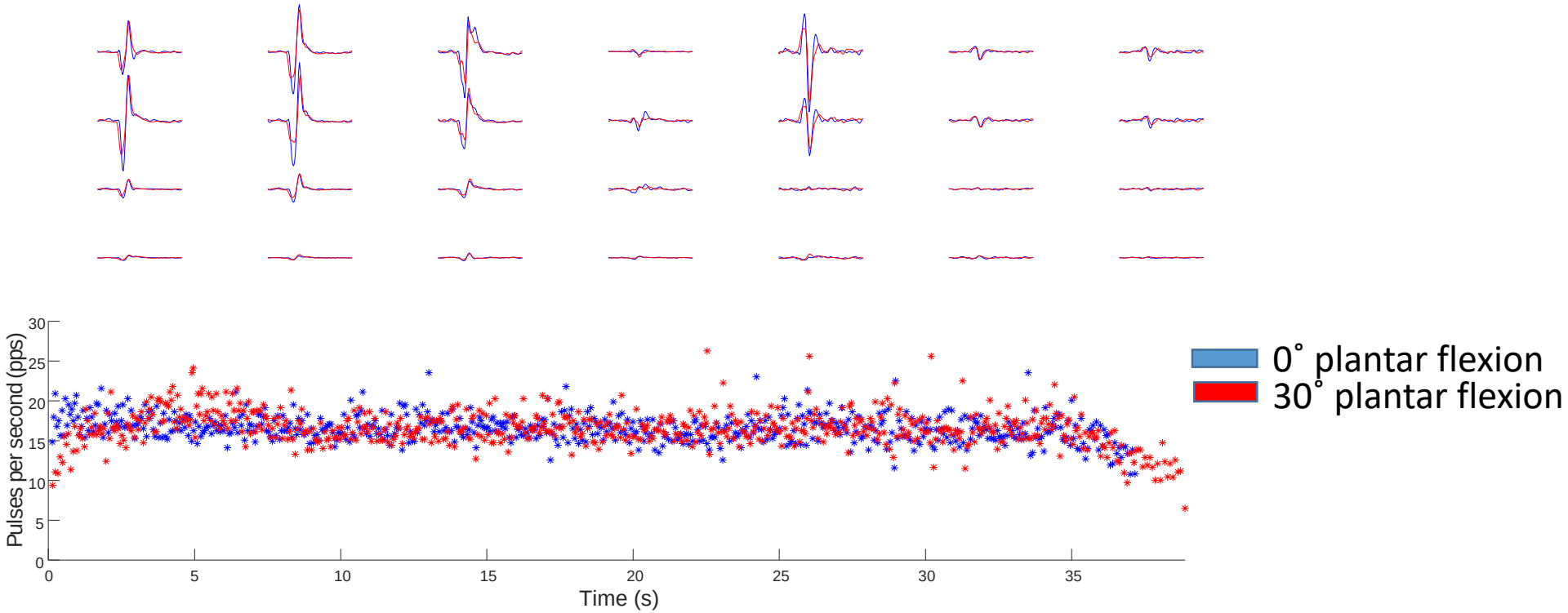

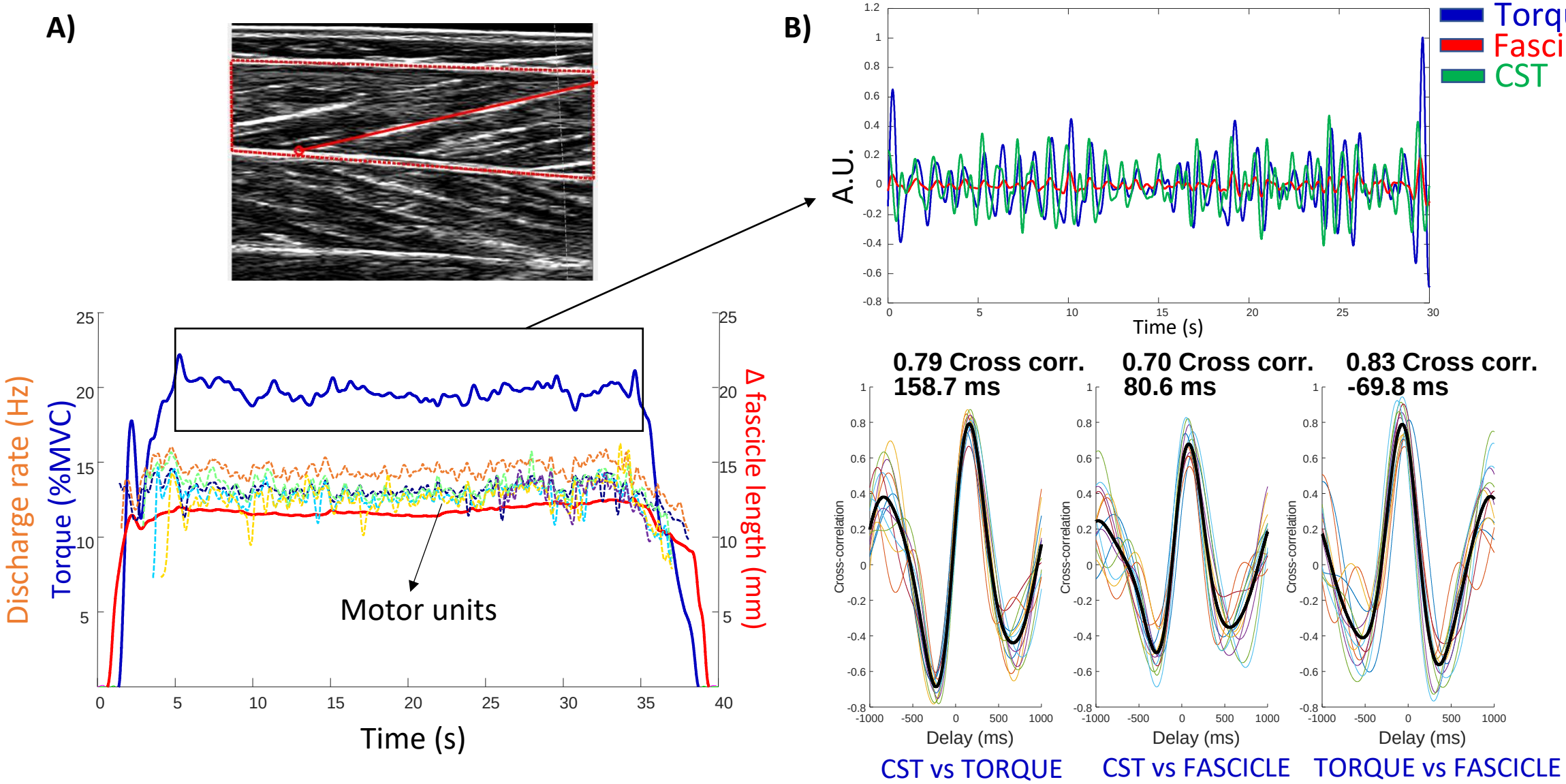
A)
B)
Torque
Fascicle
CST
A.U.
Time (s)
Discharge rate (Hz)
Torque (%MVC)
Δ fascicle length (mm)
Motor units
Time (s)
0.79 Cross corr.
158.7 ms
0.70 Cross corr.
80.6 ms
0.83 Cross corr.
-69.8 ms
Cross-correlation
Delay (ms)
CST vs TORQUE
CST vs FASCICLE
TORQUE vs FASCICLE

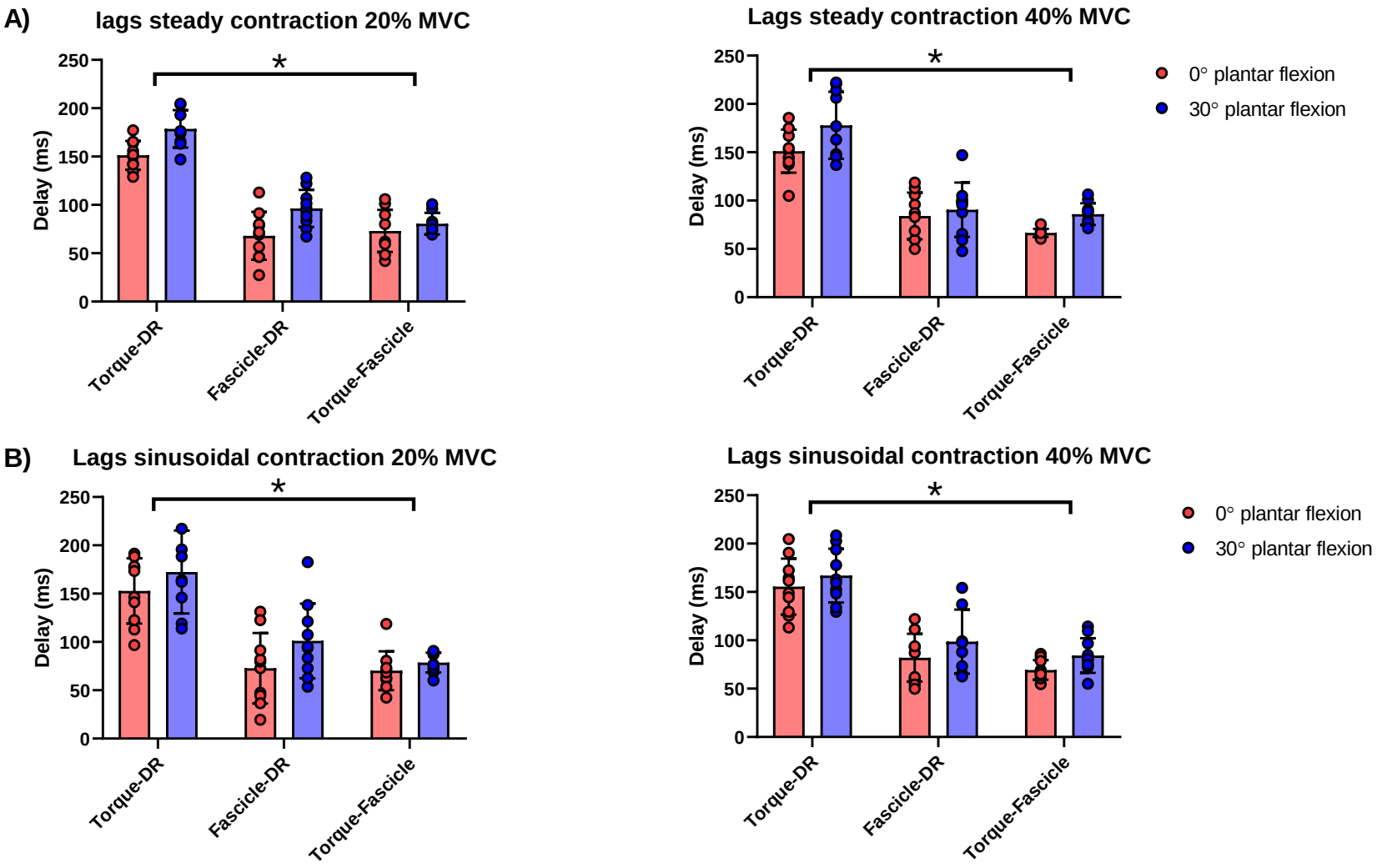
A)
lags steady contraction 20% MVC
Lags steady contraction 40% MVC
B)
Lags sinusoidal contraction 20% MVC
Lags sinusoidal contraction 40% MVC
Delay (ms)
250
200
150
100
50
0
*
Torque-DR
Fascicle-DR
Torque-Fascicle
0° plantar flexion
30° plantar flexion

A)

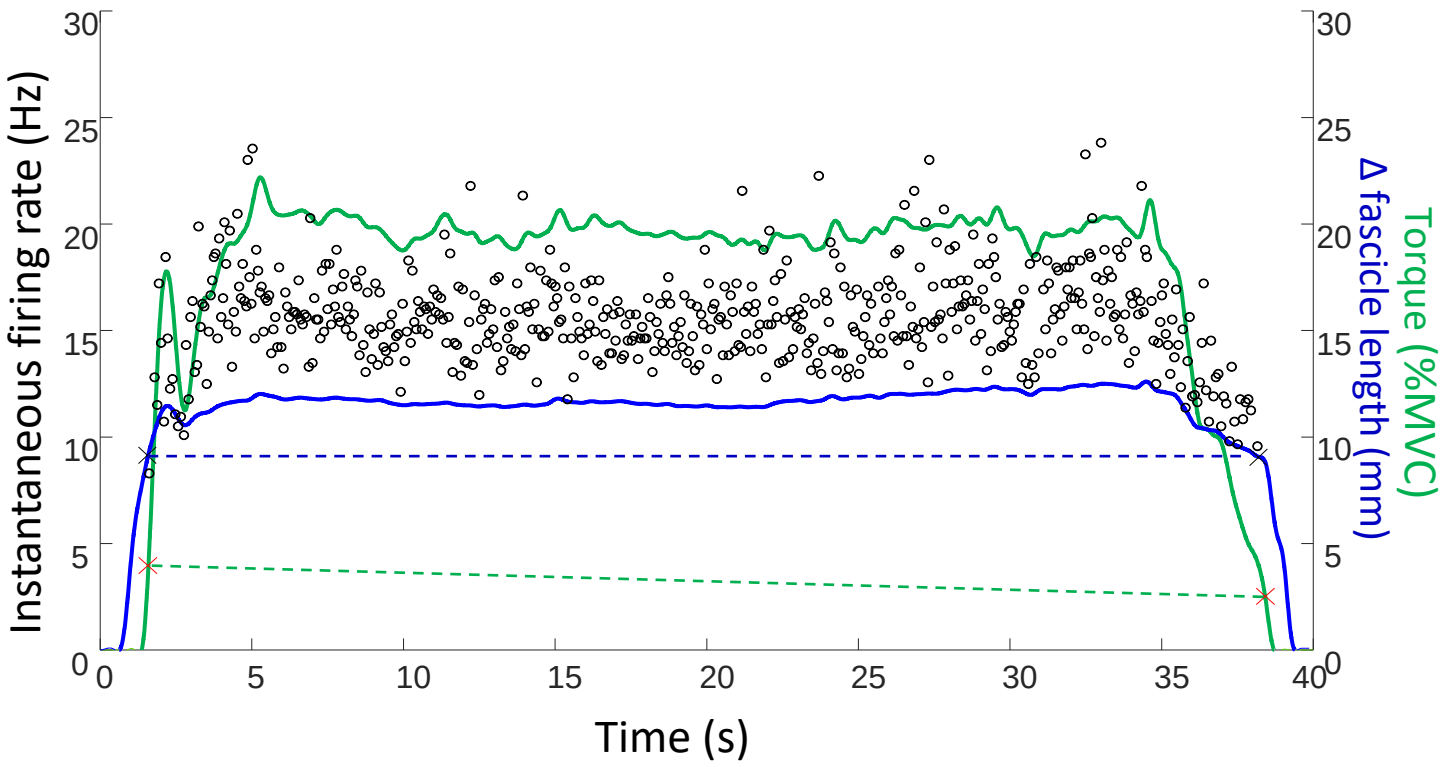
Instantaneous firing rate (Hz)
Δ fascicle length (mm)
Torque (%MVC)
Time (s)
0
5
10
15
20
25
30
35
40

B)

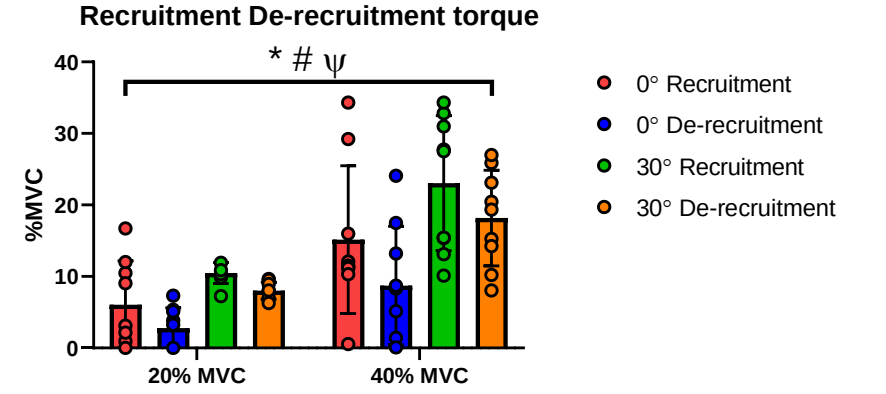
Recruitment De-recruitment torque
* # ψ
%MVC
20% MVC
40% MVC
0° Recruitment
0° De-recruitment
30° Recruitment
30° De-recruitment

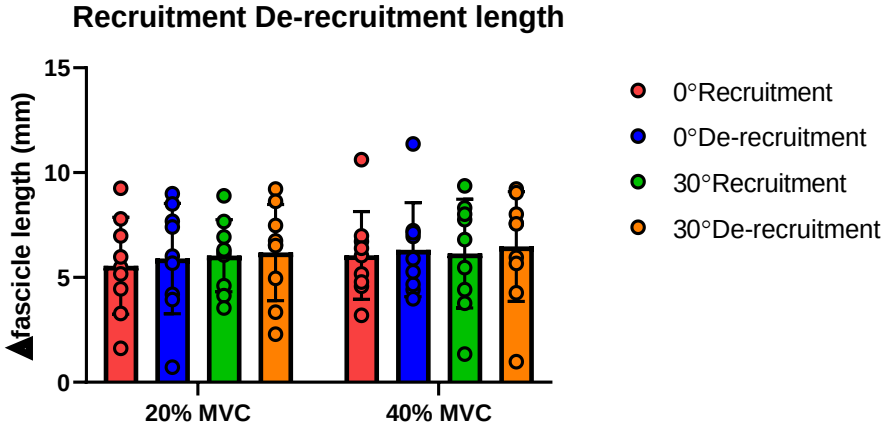
Recruitment De-recruitment length
Δfascicle length (mm)
20% MVC
40% MVC
0°Recruitment
0°De-recruitment
30°Recruitment
30°De-recruitment